

Comparison between environmental characteristics of larval bluefin tuna *Thunnus thynnus* habitat in the Gulf of Mexico and western Mediterranean Sea

Barbara A. Muhling^{1,*}, Patricia Reglero², Lorenzo Ciannelli³,
Diego Alvarez-Berastegui⁴, Francisco Alemany², John T. Lamkin⁵, Mitchell A. Roffer⁶

¹Cooperative Institute for Marine and Atmospheric Studies, University of Miami, Miami, Florida 33149, USA

²Instituto Español de Oceanografía, Centre Oceanogràfic de les Balears, Moll de Ponent s/n, 07015 Palma de Mallorca, Spain

³College of Earth, Ocean and Atmospheric Sciences, 104 CEOAS Administration Building, Oregon State University, Corvallis, Oregon 97331-5503, USA

⁴Balearic Islands Coastal Observing and Forecasting System, Parc Bit, Naorte, Bloc A 2-3, 07121 Palma de Mallorca, Spain

⁵National Oceanic and Atmospheric Administration, National Marine Fisheries Service, Southeast Fisheries Science Center, Miami, Florida 33149, USA

⁶Roffer's Ocean Fishing Forecasting Service, Inc., 60 Westover Drive, West Melbourne, Florida 32904, USA

ABSTRACT: Despite being well adapted for feeding in cold water on their North Atlantic feeding grounds, Atlantic bluefin tuna undertake long migrations to reach warm, low productivity spawning grounds in the Gulf of Mexico and Mediterranean Sea. Environmental conditions within spawning areas have been presumed to benefit larval survival, through appropriate feeding conditions, and enhanced larval retention and growth rates. However, field collections and studies to explore the potential mechanisms are rare. In this study, a comparison of the environmental characteristics of both spawning sites was completed using standardized environmental data and modeling methods. Predictive models of larval occurrence were constructed using historical larval collections, and environmental variables from both *in situ* and remotely sensed sources. Results showed that larvae on both spawning grounds were most likely to be found in warm (23 to 28°C), low chlorophyll areas with moderate current velocities and favorable regional retention conditions. In the Gulf of Mexico, larvae were located in offshore waters outside of the Loop Current and warm eddies, while in the western Mediterranean, larval occurrences were associated with the confluence of inflowing Atlantic waters and saltier resident surface waters. Although our results suggested common themes within preferred spawning grounds on both sides of the Atlantic Ocean, the ecological processes governing larval survival and eventual recruitment are yet to be fully understood.

KEY WORDS: Bluefin tuna · Spawning · Mediterranean Sea · Gulf of Mexico

— Resale or republication not permitted without written consent of the publisher —

INTRODUCTION

Spawning strategies of marine fishes frequently appear to target oceanographic conditions that promote enhanced retention, survival and eventual recruitment of larvae. This may be through favorable feeding conditions, low densities of planktonic pre-

dators, local retention or delivery towards nursery grounds, or by providing suitable temperatures for hatching, growth and larval development. Such strategies differ markedly depending on the ecology and life history of the species and the characteristics of the nursery habitat to which post-larvae must recruit. For example, several cold-water fishes in the

*Email: barbara.muhling@noaa.gov

North Atlantic Ocean spawn within the Georges Bank Gyre during the spring plankton bloom to align larvae with favorable feeding conditions and promote larval retention (Sherman et al. 1984). Atlantic herring also spawn in concert with oceanographic retention features, which may maximize return of larvae to nursery habitats (Sinclair & Iles 1985). Along upwelling coasts, species may spawn upstream of favorable larval feeding areas (Roy 1998, Landaeta & Castro 2002), or during times of low upwelling activity to maximize coastal retention (Castro et al. 2000, Shanks & Eckert 2005). Temperature-sensitive species may spawn in areas of locally enhanced production once suitable water temperatures are reached (Motos et al. 1996), while others migrate to spawning grounds based on temperature cues (Sims et al. 2004) and other cues (Cury 1994, Corten 2001).

Atlantic bluefin tuna *Thunnus thynnus* (BFT) is a highly migratory species that travels long distances between cold-water foraging areas and warm, oligotrophic spawning areas (Block et al. 2005, Rooker et al. 2007, Galuardi et al. 2010). Adult fish consume cephalopods and small benthic and pelagic fishes as prey while on feeding grounds in the North Atlantic Ocean (Chase 2002, Estrada et al. 2005). They are capable of diving to depths of up to 1000 m in waters as cold as 3°C to exploit this prey (Block et al. 2001, Walli et al. 2009). The unique circulatory system of adult BFT allows them to keep their muscles, eyes, brain and viscera warmer than ambient water temperatures, which has facilitated their expansion into cold northern Atlantic waters (Graham & Dickson 2004, Fromentin & Powers 2005). At present, although they are capable of transatlantic migrations, BFT in the North Atlantic are managed as 2 separate stocks (Block et al. 2005, International Commission for the Conservation of Atlantic Tunas 2011). The western stock generally feeds in the Northwest Atlantic, and spawns in the Gulf of Mexico (GOM) during the spring (Stokesbury et al. 2004). The eastern stock has feeding grounds off Portugal, Morocco and the Bay of Biscay, although some fish also appear to share northwestern Atlantic feeding grounds with fish from the western stock (Block et al. 2005, Fromentin & Powers 2005). All adult fish from the eastern stock are presumed to spawn in the Mediterranean Sea during the summer (Oray & Karakulak 2005, Rooker et al. 2008, Alemany et al. 2010).

Despite being well designed for life in cold waters, adult BFT migrate long distances to reach warm, oligotrophic seas in which to spawn. Arrival and residency on spawning grounds varies greatly: not all

fish appear to migrate each year (Wilson et al. 2005), and those that do can spend as little as 2 wk in spawning areas or as much as several months (Block et al. 2001, Galuardi et al. 2010). As the spawning season progresses, water temperatures on spawning grounds can warm to >28°C. Although well adapted to cold waters, BFT are not well suited for very warm waters. As temperatures approach 30°C, their cardiac function may be inhibited and they require very large amounts of oxygen to survive (Blank et al. 2004). In addition, feeding conditions for adult fish may be poor compared with North Atlantic feeding grounds, as both the GOM and Mediterranean Sea are oligotrophic in offshore waters, and low in primary and secondary productivity (Azov 1991, Estrada 1996, Gilbes et al. 1996). Despite these limitations, adult BFT migrate long distances to reach these spawning grounds. This implies that environmental conditions on spawning grounds are beneficial for larval survival.

Some previous studies examining the associations between larval BFT distributions and environmental conditions have been completed using different methodologies and different environmental predictors. These analyses found that BFT larvae tended to be located within particular oceanographic zones. In the western Mediterranean Sea, larvae were most abundant near the salinity front where inflowing Atlantic waters converge with higher salinity resident waters around the Balearic Islands (Garcia et al. 2005, Alemany et al. 2010, Reglero et al. 2012). Larvae have also been collected in other regions within the Mediterranean Sea, mainly in the central Mediterranean around Sicily and other smaller islands, in areas also characterized by the confluence of inflowing surface Atlantic waters and saltier resident waters (Tsuji et al. 1997, Koched et al. 2012). More recently, BFT larvae have been found near Cyprus (Oray & Karakulak 2005). However, these were assumed to come from a resident subpopulation that does not migrate out of the Mediterranean Sea. In the GOM, BFT larvae were found most frequently in 'common waters' outside of the warm Loop Current and associated warm-core rings, and away from higher chlorophyll continental shelf waters (Muhling et al. 2010, Lindo-Atichati et al. 2012). Spawning seasons in both regions appeared likely to extend for around 6 to 8 wk, and were closely tied with sea temperatures (Muhling et al. 2010). These results contrast with the more protracted spawning of tropical tunas, which can last for more than 6 mo of the year (Schaefer 2001). However, a direct comparison of conditions on the 2 spawning grounds, using the

same environmental variables and the same methods, is lacking.

Despite their considerable commercial value, our understanding of the ecological drivers of migration and spawning behavior in adult BFT is limited. The reasons why adult BFT expend large energy reserves to migrate to spawning locations that they find physiologically stressful remain unclear. By comparing and contrasting the environmental conditions at spawning grounds on both sides of the Atlantic Ocean, the general conditions adult fish appear to target for spawning can be defined. In addition, we can begin to define relationships between larval occurrences and the physical environment, and distinguish between those that are probably due to physiological constraints and those that are proxies for other factors, such as water mass or feeding ecology. Improving our understanding in these areas will also allow existing indices of abundance used in stock assessments to be refined (Ingram et al. 2010). In the future, inferences can be drawn about factors influencing recruitment, potential responses to climate change and the implications of management actions (Garcia et al. 2013).

In this study, we used the same environmental variables and modeling methods to define the environmental characteristics of larval BFT collection locations in the northern GOM and the western Mediterranean Sea. Larval occurrence models were constructed using historical larval survey data and environmental variables from both *in situ* CTD casts and remotely sensed satellite data. We aimed to compare and contrast conditions at each sampling site, and to use those results to consider the potential ecological requirements that may benefit larval survival.

MATERIALS AND METHODS

Larval surveys

Larval BFT were collected in the northern GOM through the National Marine Fisheries Service Southeast Area Monitoring and Assessment (SEAMAP) Program (Fig. 1, Table 1). Data were available

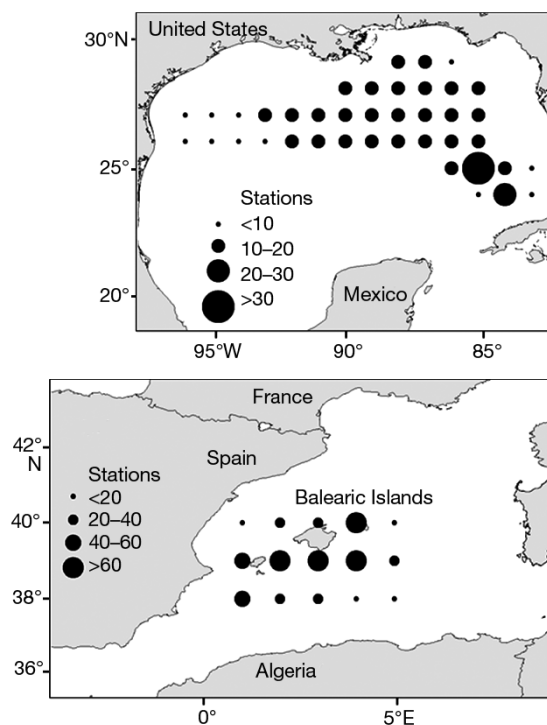


Fig. 1. Sampling areas in the Gulf of Mexico, 1998 to 2009 and Balearic Islands, 2001 to 2005. Sample sizes of stations are shown on a one degree squared grid, and summed to show sampling effort

Table 1. No. of stations with all environmental variables available, and the dates they were sampled in the Gulf of Mexico (GOM) and Balearic Islands (BI), 1998 to 2009. Mean no. of Atlantic bluefin tuna *Thunnus thynnus* (BFT) larvae per 10 m² is also shown for each sampled year (bongo nets only), with standard errors in parentheses

Year	GOM start	GOM end	No. of GOM stations	GOM mean per 10 m ² (SE)	BI start	BI end	No. of BI stations	BI mean per 10 m ² (SE)
1998	26 April	30 May	47	1.05 (0.66)				
1999	24 April	30 May	61	1.18 (0.48)				
2000	20 April	25 May	62	3.16 (1.58)				
2001	18 April	27 May	61	5.99 (2.34)	16 June	7 July	114	3.48 (1.07)
2002	19 April	28 May	50	3.00 (1.51)	7 June	26 June	55	4.59 (2.01)
2003	13 May	30 May	42	3.97 (1.50)	4 July	29 July	117	5.44 (2.51)
2004	6 May	30 May	30	6.14 (3.50)	18 June	10 July	154	7.94 (5.68)
2005					28 June	23 July	159	2.79 (0.75)
2006	24 April	28 May	66	1.51 (0.54)				
2007	18 April	23 May	35	3.62 (1.82)				
2008	21 April	30 May	56	1.57 (0.58)				
2009	14 May	31 May	20	12.99 (4.80)				

for 1982 to 2009, although only data from 1998 to 2009 were used for habitat modeling, to align with the remotely sensed chlorophyll record (see below). Oblique bongo and surface neuston tows were conducted as described in Scott et al. (1993) and Muhling et al. (2010) across a grid of stations completed between mid April and the end of May each year. Bongo nets were fitted with a 333 μm mesh on two 61 cm diameter round frames and towed obliquely to 200 m depth, or to within 10 m of the bottom in shallower water. Neuston nets were fitted with 0.95 mm mesh on a 1 \times 2 m frame, and were towed at the surface. Samples from the right bongo net and the neuston net were sorted, and larvae identified to the lowest possible taxa at the Polish Plankton Sorting and Identification Center in Szczecin, Poland. The identifications of all scombrid larvae were confirmed at the Southeast Fisheries Science Center in Miami, Florida.

In the western Mediterranean Sea, larval BFT were collected during 5 annual surveys completed from 2001 to 2005 during June and July around the Balearic Islands (BI) (Fig. 1, Table 1). The area covered by these surveys was less than in the northern GOM (~180 \times 220 n mile vs. ~700 \times 330 n mile). However, station spatial density was greater, with between 185 and 221 stations per annual survey vs. between 31 and 81 stations in the GOM (Alemany et al. 2010, Reglero et al. 2012). Similar to the GOM surveys, larvae were collected with bongo nets of 60 cm diameter, however nets were towed obliquely to only 70 m depth around the BI (vs. 200 m in the GOM). During the first 2 yr of surveys around the BI, both nets were fitted with a 250 μm mesh, and from 2003 onwards, one net was 200 μm (not sorted for larvae) and one was 333 μm (used for larval collections). Larvae were removed from plankton samples and identified to species level. In the GOM, between 20 and 66 stations per year were available with all environmental variables present, with between 55 and 159 per year in the BI (Table 1).

Environmental variables

A suite of environmental variables were selected for inclusion in predictive habitat models. Temperature is an important physiological control of many biological processes, including spawning (e.g. Masuma et al. 2006), and so temperatures at 3 discrete depths (0, 100 and 200 m) were included. In addition to temperature, salinity is an effective tracer of water mass, and so this variable was also included at the

same 3 depths. Chlorophyll is a proxy for primary productivity, so surface chlorophyll values available from remotely sensed data were incorporated. Geostrophic velocities can highlight broad frontal zones and regions of different retention conditions. Finally, larval behaviors and catchability may follow a diel cycle in some species, and so time of day was also included in habitat models.

In both the northern GOM and BI surveys, *in situ* hydrographic data were collected using a Seabird SBE 9/11 CTD with temperature, pressure, conductivity and dissolved oxygen sensors. Temperature and salinity at the surface (mean of upper 5 m), 100 and 200 m depth were available for the majority of sampled stations, and were chosen as representative depths for analysis. Temperature at the surface is influenced by seasonal warming, while salinity at the surface is primarily affected by riverine outflow in the GOM, and the inflow of Atlantic Ocean waters in the BI. Physical measurements at 100 and 200 m depth were chosen to indicate water mass structure and subsurface features. While water masses in the BI region can frequently be differentiated by surface variables, particularly salinity, the GOM becomes largely isothermal by late spring, and water masses are much more easily defined at depth.

Remotely sensed variables

Reliable *in situ* measurements of chlorophyll *a* were not available for both surveys, so remotely sensed data were used instead. Surface chlorophyll values in mg m^{-3} were extracted for each station date and location from 8 d composites of data from 2 sensors: Sea-viewing Wide Field-of-view Sensor (SeaWiFS) and Moderate Resolution Imaging Spectroradiometer (MODIS)-Aqua. Level 3 Standard Mapped Image products published by NASA's Goddard Space Flight Center OceanColor Group were selected for use. SeaWiFS data were available from 1998 to 2010, with some periodic data gaps from satellite outages in more recent years. MODIS-Aqua data were available from 2003 onwards. Composites of 8 d were chosen as a suitable compromise between spatial and temporal accuracy, and minimizing cloud impacts. Data values were extracted using the Marine Geospatial Ecology Toolbox (MGET, Roberts et al. 2010) in ArcGIS 9.3 (Esri). Where data from only one sensor were available for a particular station, that value was used, and where data from both sensors were available, a mean was taken. Correlations between values from the 2 sensors were strong in both

the GOM (Pearson's $r = 0.8$), and the BI (Pearson's $r = 0.86$).

Geostrophic velocity in the GOM was obtained from daily Aviso global altimetry data at a spatial resolution of approximately 0.333° , and extracted in ArcGIS using the MGET toolbox. Owing to the presence of islands and complex mesoscale flows, geostrophic velocity measurements around the BI were best obtained from *in situ* measurements (Reglero et al. 2012). In this region, geostrophic velocity was estimated by differentiating the interpolated dynamic height field, which was calculated from CTD data (Torres et al. 2011). These data had a variable spatial resolution, depending on the sampling grid, but averaged approximately 0.167° .

Modeled climatologies

Climatologies of temperature and salinity at the surface and 100 m depth, surface chlorophyll and surface current velocities were constructed to better visualize typical oceanographic conditions in each region at the time of peak spawning. Surface chlorophyll climatologies were constructed using MODIS-Aqua data, while temperature and salinity climatologies were constructed using the HYbrid Coordinate Ocean Model (HYCOM) + Navy Coupled Ocean Data Assimilation (NCODA) Global 1/12 Degree

Analysis (GLBa0.08). Although HYCOM performed quite well in replicating observed temperature and salinity fields in both regions, and surface current fields in the GOM, it was less successful for estimating surface currents in the BI region. For this reason, mean geostrophic currents from Aviso mean absolute dynamic topographies were used for climatologies of surface currents in both regions, despite lower spatial resolution. Spawning peaks around the second half of May in the GOM (Muhling et al. 2010) and in early July in the BI region, so these months were chosen for climatological analyses. Data from 2003 to 2012 were used for each climatology, all of which were compiled using MGET in ArcGIS.

Habitat models

Habitat models were constructed by combining all 8 environmental variables (surface temperature, salinity, chlorophyll, temperature and salinity at 100 and 200 m depth, geostrophic currents) with day of the year and hour of sampling, into multivariate predictive habitat models. An initial problem with the input variables was the high degree of collinearity (Table 2). This can result in model non-convergence, inconsistent results and degraded model performance (Walczak & Cerpa 1999, Neumann 2002). Patterns of collinearity differed between the 2 regions.

Table 2. Pearson correlations among environmental variables within the Gulf of Mexico (GOM) and Balearic Islands (BI). SS denotes sea surface, or 0 m depth, T is temperature, S is salinity, Chl is chlorophyll *a* and GeoVel is geostrophic velocity. Correlations >0.5 are shown in bold

	SST	SSS	T100m	S100m	T200m	S200m	Yearday	Hour	Chl
GOM									
SSS	0.04								
T100m	0.51	0.10							
S100m	0.00	0.30	-0.08						
T200m	0.41	0.09	0.90	-0.13					
S200m	0.25	0.22	0.67	0.26	0.72				
Yearday	0.49	-0.05	0.02	0.06	-0.02	-0.01			
Hour	0.07	-0.01	0.02	0.01	0.01	0.03	-0.01		
Chl	-0.28	-0.46	-0.31	-0.05	-0.28	-0.26	-0.01	-0.03	
GeoVel	0.40	0.12	0.60	0.09	0.47	0.48	-0.14	0.08	-0.25
BI									
SSS	0.12								
T100m	-0.02	-0.64							
S100m	-0.04	0.65	-0.69						
T200m	-0.03	-0.51	0.56	-0.40					
S200m	0.02	0.33	-0.36	0.67	0.20				
Yearday	0.88	0.26	-0.05	0.12	-0.05	0.16			
Hour	0.02	-0.10	0.03	-0.04	0.03	-0.04	-0.06		
Chl	-0.19	0.12	-0.20	0.11	-0.22	-0.08	-0.27	-0.03	
GeoVel	-0.01	-0.22	0.28	-0.19	0.06	-0.17	-0.07	0.08	-0.04

In the BI, surface salinity was correlated with temperature and salinity at depth, and surface temperatures were also strongly correlated with day of the year (Table 2). However, in the GOM, temperature and salinity at depth were strongly correlated with each other. To address this problem, we followed the approach of Malmgren & Winter (1999) and Sousa et al. (2007), and used principal component analysis (PCA) to reduce the dimensionality of the environmental variable matrix and provide a new set of uncorrelated axes. PCA was applied to a Euclidean distance matrix of normalized environmental data from each region separately in Primer-6 software (Clarke & Gorley 2006), with all environmental variables included. Resulting principal component axes were then input as predictor variables to a multilayer perceptron artificial neural network model to provide estimates of larval BFT distributions and define environmental conditions in both regions where larvae have been most likely to be collected historically.

Artificial neural networks are flexible and accurate predictive models that do not require normally distributed data and can model highly nonlinear functions. They generally perform well for addressing questions related to species distribution modeling (Segurado & Araujo 2004). Models learn by self-adjusting a set of parameters, and then using an algorithm to minimize the error between the desired output (observed) and the network output (predicted) (Malmgren & Winter 1999). Multilayer perceptron neural networks consist of systems of interconnected nodes with an input layer, a hidden layer and an output layer, with each layer containing one or more neurons. Each layer is connected by nonlinear transfer functions (Gardner & Dorling 1998). The input layer contains one neuron for each predictor variable. The hidden layer contains a variable number of neurons: more neurons tend to improve model fit, however too many can lead to overfitting, thus internal model validation is required (Olden et al. 2008). In this study, overfitting was prevented by holding back 20% of training data rows as the model fit was being performed and continually evaluating model fit against the hold-out dataset (Sherrod 2003). The neural networks used were supervised, feed-forward models with one hidden layer, trained by a conjugate gradient back-propagation algorithm. These types of neural networks are popular in ecology because they can approximate any continuous function (Olden et al. 2008). Logistic functions were used for hidden- and output-layer activation (Sherrod 2003), and v-fold cross validation was used for model testing and validation. The relative importance of each

predictor variable was calculated using sensitivity analysis, where the values of each variable are randomized and the effect on the quality of the model is measured (Sherrod 2003). Variables not contributing to a final model are excluded. This process results in a score out of 100 for each predictor variable, with 100 always denoting the most important predictor. A separate model was constructed for each sampled region (GOM and BI), using DTREG software (Sherrod 2003).

As BFT larval abundances were often low and variable, and the sampling gears between regions were not directly comparable, models were constructed to predict the presence or absence of BFT larvae, rather than abundance. Net tows in the GOM were much deeper than in the BI (200 vs. 70 m depth). Larval BFT are usually most abundant in the upper 10 to 20 m of the water column (Muhling et al. 2012), so the GOM surveys probably underestimated the presence of BFT larvae substantially. To partially account for this, if either or both gears (bongo or neuston) at each station in the GOM caught BFT larvae, the station was considered to be a 'positive' station (see Muhling et al. 2010). Recent experiments using a gear more comparable to the technique used in the BI show the validity of this methodology (Muhling et al. 2012). To compensate for this potential difference in catchability between regions, and general expected inefficiencies in sampling of rare larvae due to gear avoidance, misclassification costs were assigned to each model from each region (Sherrod 2003). This parameter was adjusted in an iterative fashion, and set at the lowest possible value at which model sensitivity remained above 80% (Muhling et al. 2010).

To investigate the relationships between model predictions and the raw environmental variables, scatterplots between each variable and the predicted probability of larval occurrence from each neural network model were constructed. Although these plots did not take into account interactions among variables, they provided an indication of which variables were most important in predicting suitable habitat. In addition, they showed the nature of the relationship between larval occurrences and each variable (i.e. positive, negative, parabolic), using polynomial lines of best fit. Observed proportions of positive stations for each variable, divided into bins, were overlaid on the scatterplots.

To briefly investigate potential interactions among variables, wireframe contour plots of modeled probabilities of occurrence were constructed for 2 influential environmental variables, for each study region. As each neural network model ranked the input vari-

ables (i.e. principal component axes) in terms of contribution to the model, we selected an environmental variable strongly correlated with the most important, and second most important, input principal component axis for each model for inclusion in the wire-frame plots.

Generated probabilities of occurrence from neural network models from 2 selected from each region were contoured across each sampling area, using kriging in Surfer 9 (Golden Software), and BFT larvae catch locations for each of these years were overlaid. We selected 2 years from each region with differing oceanographic conditions to investigate if and how larval occurrences moved with oceanographic features.

RESULTS

Regional oceanographic conditions

The GOM during May was typically cooler in surface waters on the continental shelf than offshore, and warmer within the main body of the Loop Cur-

rent (Fig. 2). Surface salinities on the shelf were lower than in the open GOM, in association with riverine outflow. At depth, both temperature and salinity were higher within the Loop Current and in the general position of large anticyclonic rings, which are periodically shed from the current. Surface chlorophyll was highest on the continental shelf, and lowest within the Loop Current region. Surface current velocities were markedly higher in the area of influence of the Loop Current, from the western Caribbean Sea through to the eastern GOM and Florida Straits (Fig. 2).

Surface temperatures during July in the western Mediterranean Sea were warmest off the coasts of Spain and Algeria, and around the BI (Fig. 3). Cooler waters were associated with the south coast of France. Salinities at the surface and at depth were lowest in the western portion of the study area, in association with inflow of Atlantic water. Temperature at depth was spatially variable, with maximum values off the northern African coast. Similar to the GOM, surface chlorophyll was generally low, with higher values near the south coast of France. Surface current velocities were highest in the Alboran Sea,

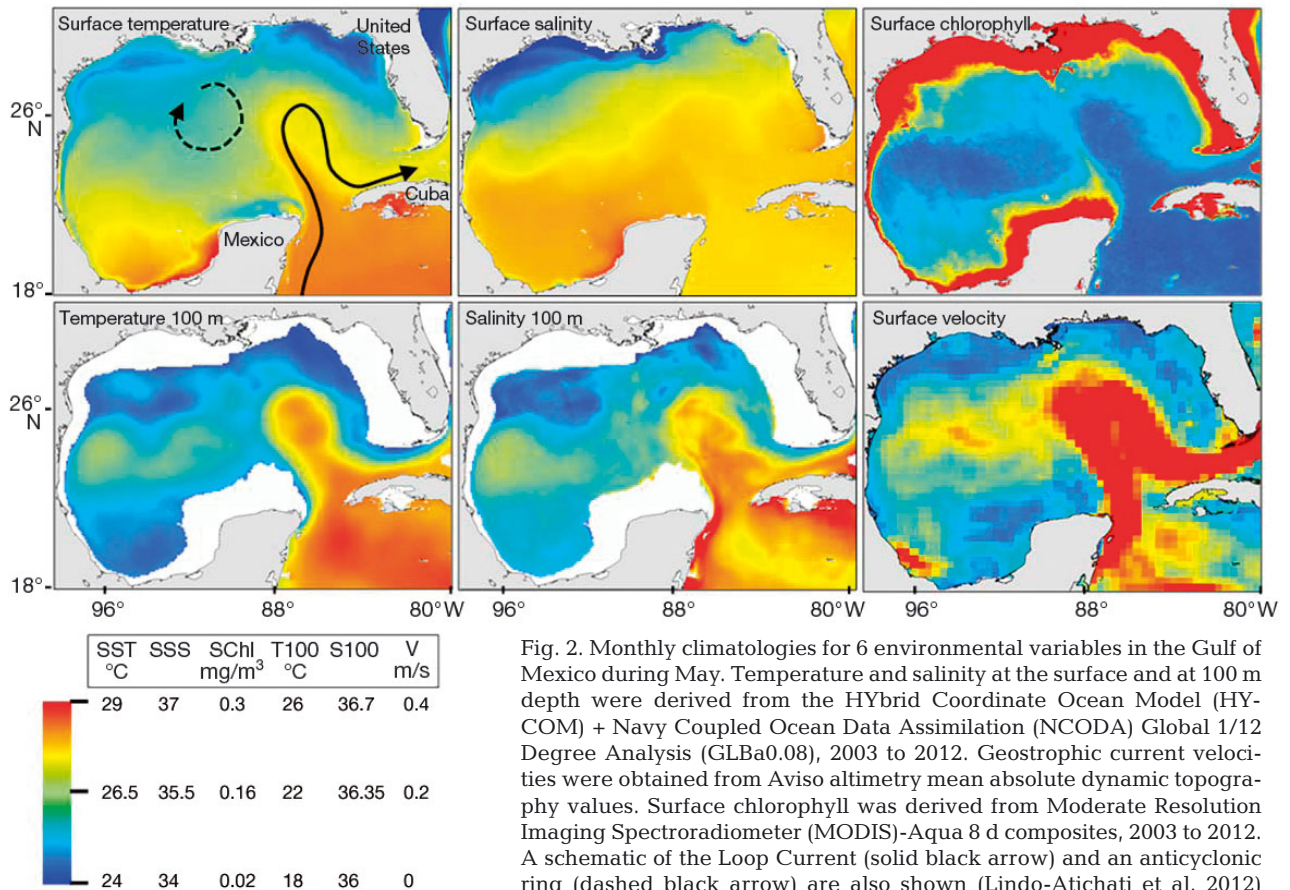


Fig. 2. Monthly climatologies for 6 environmental variables in the Gulf of Mexico during May. Temperature and salinity at the surface and at 100 m depth were derived from the HYbrid Coordinate Ocean Model (HYCOM) + Navy Coupled Ocean Data Assimilation (NCODA) Global 1/12 Degree Analysis (GLBa0.08), 2003 to 2012. Geostrophic current velocities were obtained from Aviso altimetry mean absolute dynamic topography values. Surface chlorophyll was derived from Moderate Resolution Imaging Spectroradiometer (MODIS)-Aqua 8 d composites, 2003 to 2012. A schematic of the Loop Current (solid black arrow) and an anticyclonic ring (dashed black arrow) are also shown (Lindo-Atichati et al. 2012)

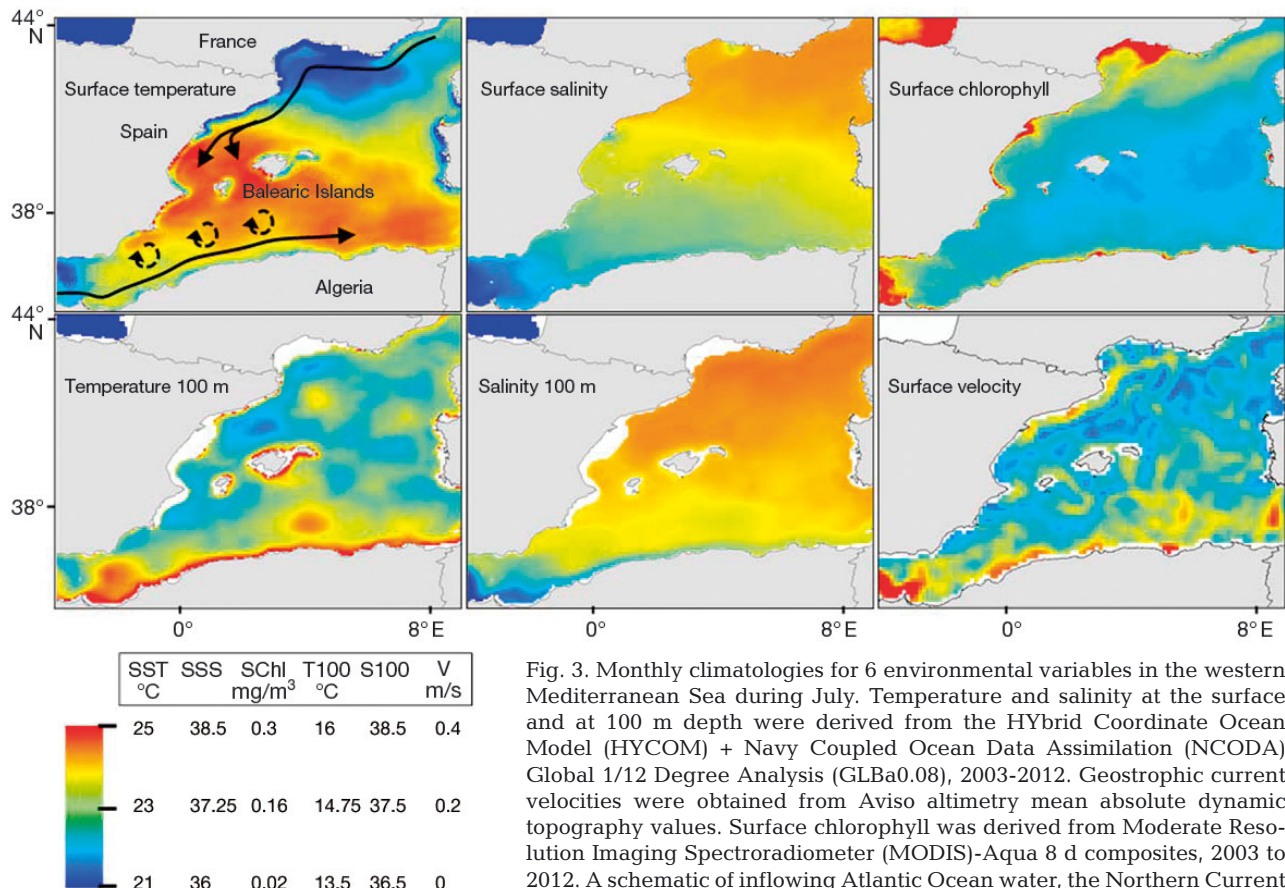


Fig. 3. Monthly climatologies for 6 environmental variables in the western Mediterranean Sea during July. Temperature and salinity at the surface and at 100 m depth were derived from the HYbrid Coordinate Ocean Model (HYCOM) + Navy Coupled Ocean Data Assimilation (NCODA) Global 1/12 Degree Analysis (GLBa0.08), 2003-2012. Geostrophic current velocities were obtained from Aviso altimetry mean absolute dynamic topography values. Surface chlorophyll was derived from Moderate Resolution Imaging Spectroradiometer (MODIS)-Aqua 8 d composites, 2003 to 2012. A schematic of inflowing Atlantic Ocean water, the Northern Current along the French coast (black arrows) and regions of typical mesoscale eddy activity (dashed black arrows) are also shown (Reglero et al. 2012)

and along the northern coast of Algeria (Fig. 3). Moderate mean currents were also observed north of the BI, however, in general, velocities in the BI region were much lower than in the Alboran Sea, and also lower than in the Loop Current area of influence in the GOM.

Larval habitat models

On a weekly basis, the proportion of sampled stations with >0 BFT larvae increased with increasing surface temperatures within both study regions (Fig. 4). Occurrences of larvae in the GOM increased from around 5% in mid April to 35% towards the end of May. Samples from 1998 to 2009 were available only until the end of May, however the proportion of positive stations from historical data (1982 to 2009) included some June stations, which are also shown in Fig. 4. During the sampled time period, surface temperatures from CTD casts at sampled stations increased from a mean of ~24.5°C to 27°C, although

variability around these means was high. In the BI region, the proportion of positive stations increased from ~5% in early-mid June to a peak of 20 to 25% by the first week of July. Larval occurrences then decreased back to around 5% by the end of July. During this 8 wk period, mean surface temperatures at sampled stations increased from less than 21°C to greater than 27°C. Spawning in the BI region thus tended to begin at cooler temperatures than in the GOM, but the rate of temperature increase through the sampling period was higher (Fig. 4).

PCA analysis of environmental conditions at each sampled station in each region showed a general separation of water mass along the first principal component, PC1 (Fig. 5). In the GOM, stations with negative values along PC1 had higher temperatures at 100 and 200 m depth, higher salinity at 200 m, higher geostrophic velocities and low surface chlorophyll. These stations were probably associated with the Loop Current or warm rings of Loop Current origin. Along the second principal component, PC2, stations with positive values were sampled later in the

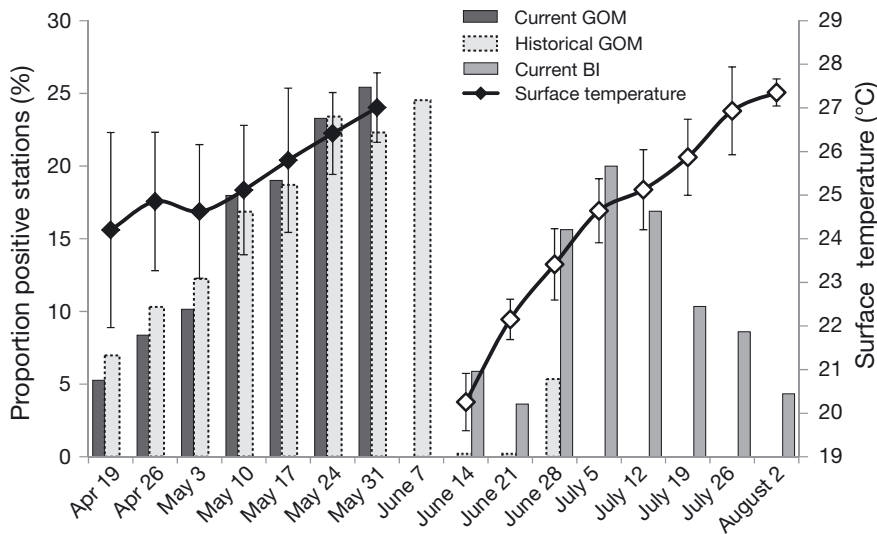


Fig. 4. Proportion of stations with >0 bluefin tuna larvae by week for the Gulf of Mexico (GOM, 1998 to 2009) and Balearic Islands (BI, 2001 to 2005). Proportions were calculated for all stations sampled during each week, for all sampled years together. Gray dashed series shows the proportion of positive stations by week for the GOM for the years 1982 to 2009, to show results from some June samples collected in the mid 1990s. Mean (\pm SD) surface temperatures from CTD casts taken at sampled stations are also shown. \blacklozenge : GOM; \diamond : BI

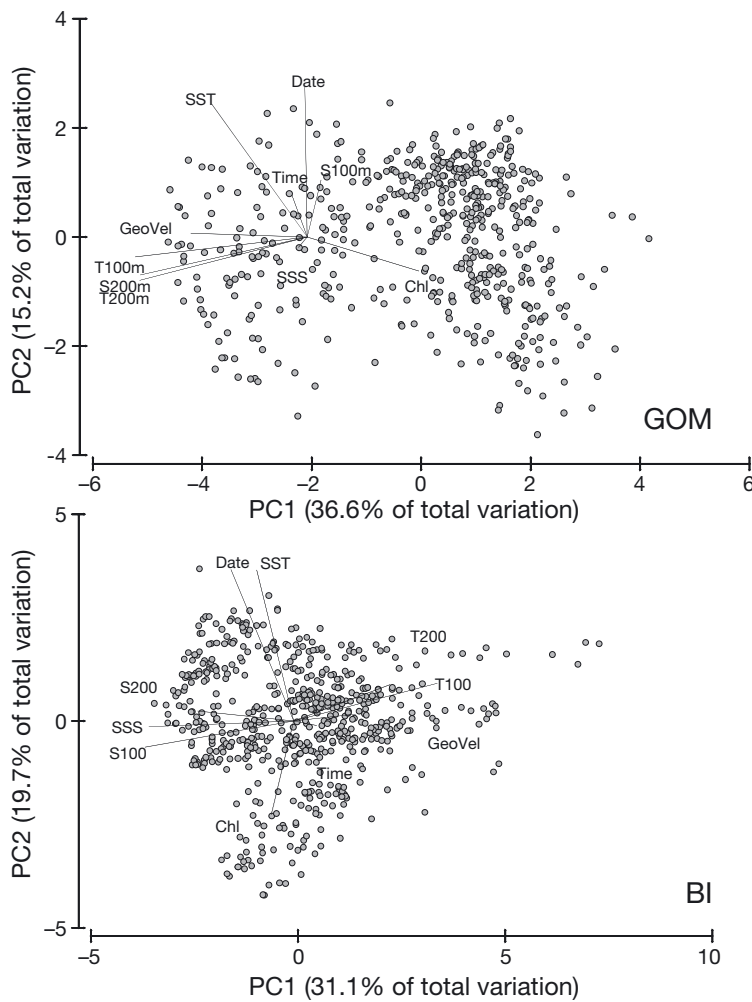


Fig. 5. Principal component (PC) analysis on 10 environmental variables from the Gulf of Mexico (GOM) and Balearic Islands (BI). Vectors of each variable are shown, where T is temperature, S is salinity, Chl is chlorophyll *a* and GeoVel is geostrophic velocity. The first two principal component axes are shown, along with the percent of total variation explained by each axis

year, and showed higher surface temperatures. In the BI, stations with positive values along PC1 had higher temperatures at depth, and lower salinities throughout the water column. These stations were probably associated with inflowing Atlantic water. Along PC2, stations with positive values were sampled later in the year, and showed higher surface temperatures along with lower surface chlorophyll (Fig. 5).

In both regions, 6 principal component axes encompassed more than 90% of the sample variability, and so the first 6 axes from each PCA analysis were input to neural network models (Table 3). In the GOM, PC2 was the most important variable, suggesting a strong influence of date and surface temperature. In the BI, PC1 was the most influential predictor, implying that water mass was the most important consideration when predicting larval occurrences. In the GOM, the strong influence of day of the year was apparent, with generally increasing probabilities of occurrence through time. This trend was also evident from a histogram of positive stations through time from the raw data (Fig. 6). Predicted and actual probabilities of larval occurrence decreased with increasing salinity and temperature at depth, suggesting lower occurrences within Loop Current waters. The relationship between larval occurrences and surface temperatures was parabolic, with maximum probabilities of occurrence between 25 and 27°C. In the BI, day of the year was also

Table 3. Cumulative variation explained by first 6 principal component (PC) axes for the Gulf of Mexico (GOM) and Balearic Islands (BI). Correlations among each axis and each environmental variable are also shown, where SS denotes sea surface, or 0 m depth, T is temperature, S is salinity, Chl is chlorophyll *a* and GeoVel is geostrophic velocity. The importance of each axis in the neural network model is shown as a score out of 100, with higher values denoting greater importance in the model

	Cumulative variation explained (%)	SST	SSS	T100m	S100m	T200m	S200m	Chl	GeoVel	Yearday	Hour	Variable importance
GOM												
PC1	36.60	-0.53	-0.05	-0.95	0.08	-0.92	-0.92	0.61	-0.64	-0.01	-0.08	67.58
PC2	51.82	0.73	-0.06	-0.11	0.31	-0.24	-0.21	-0.19	0.02	0.83	0.23	100.00
PC3	65.95	-0.07	0.83	-0.09	0.51	-0.18	-0.18	-0.47	0.26	-0.30	0.03	47.94
PC4	75.78	0.06	0.14	0.00	-0.09	0.02	0.01	-0.13	-0.11	0.23	-0.93	60.54
PC5	85.27	0.05	-0.38	0.08	0.69	-0.03	0.03	0.34	0.32	-0.19	-0.25	52.70
PC6	91.8	-0.19	0.06	0.12	0.39	0.18	0.22	-0.03	-0.59	0.13	0.08	22.60
BI												
PC1	31.14	-0.22	-0.84	0.83	-0.86	0.56	-0.56	-0.13	0.36	-0.36	0.13	100.00
PC2	50.82	0.88	-0.03	0.22	-0.15	0.21	0.06	-0.54	0.04	0.88	-0.03	63.37
PC3	64.39	0.26	0.14	-0.09	-0.27	-0.69	-0.75	0.31	0.18	0.13	0.04	36.52
PC4	74.57	-0.02	-0.02	0.07	-0.13	0.05	-0.11	0.10	-0.39	0.03	-0.91	3.33
PC5	83.53	0.02	-0.05	-0.07	-0.17	0.02	-0.16	-0.06	-0.82	-0.02	0.38	11.68
PC6	91.22	0.25	-0.10	0.06	-0.01	0.25	0.16	0.76	-0.03	0.13	0.10	6.07

influential, with modeled and actual probabilities of occurrence increasing through to early July, before decreasing again. Larvae were also most likely to be collected at stations with low surface chlorophyll (<~0.2 mg m⁻³), and where surface temperatures were between 24 and 26°C (Fig. 7).

Results suggested that probabilities of occurrence in the GOM peaked at surface temperatures 1 to 2°C higher than in the BI. In contrast, salinities at the surface and at depth barely overlapped between the 2 study areas, with the BI much more saline than the GOM (>36.4 vs. 34–37). The range of temperatures at 200 m depth varied to a much greater degree in the GOM (~12°C) than in the BI (~1°C). Ranges of surface chlorophyll were similar. However, although probabilities of occurrence in the BI were proportionally greater at low chlorophyll values (<~0.2 mg m⁻³), there was no strong relationship in the GOM.

The most important predictor in the GOM was PC2, which was driven by variability in surface temperature and date. However, the relationship between modeled probabilities of occurrence and surface temperature shown in Fig. 6 was weak, with high variability around the line of best fit. One possibility for this observation was an interaction between surface temperature and some other environmental variable. The second most important predictor in the GOM model was PC1, which captured water mass characteristics, such as temperature and salinity at depth. A wireframe plot of predicted probabilities of larval occurrence with both surface temperature and

temperature at 100 m depth was constructed to investigate potential interactions between surface temperature and water mass (Fig. 8). Probabilities of larval occurrence showed a parabolic relationship with surface temperature, peaking at between 25 and 28°C, however this relationship was only present where temperature at depth was less than around 22°C (i.e. outside the Loop Current). The relationship between larval occurrences and surface temperatures was thus dependent on the water mass sampled, in that the relationship between surface temperature and larval occurrences was observed only outside of Loop Current water. Within Loop Current water larval occurrences were persistently low (Fig. 8).

The most important predictor in the BI neural network model was PC1. This axis generally separated stations located in different water masses, as indicated by surface salinity and temperature and salinity at depth. The second most important predictor was PC2, which described the variability in surface temperature and date. Similar to the GOM, probabilities of larval occurrence against surface salinity and surface temperature in the BI highlighted a parabolic relationship between temperature and BFT larvae (Fig. 8). Maximum probabilities of occurrence were found between ~24 and 27°C. However, apart from a small peak of larval occurrences in cool waters with high surface salinities, there was little interaction evident between predicted probabilities with surface temperature and surface salinity in the BI (Fig. 8).

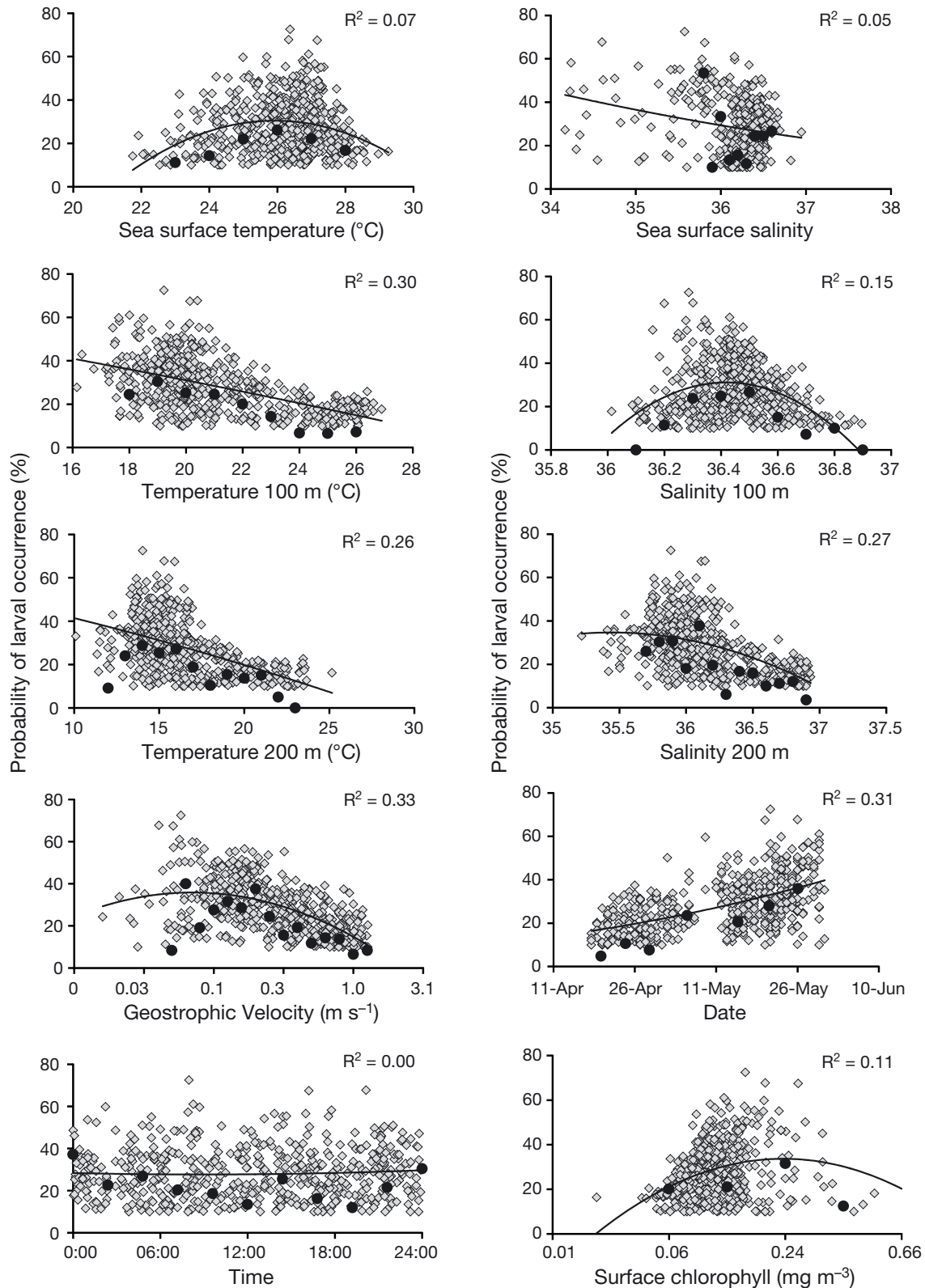


Fig. 6. Scatterplots of environmental variables and predicted probabilities of occurrence from the neural network model for the Gulf of Mexico. The general nature of the relationship between larval occurrences and each variable are shown using polynomial lines of best fit (black line). Observed proportions of stations with >0 bluefin tuna larvae are also shown in solid black dots, for binned environmental variables. Note nonlinear scales for surface chlorophyll and geostrophic velocities

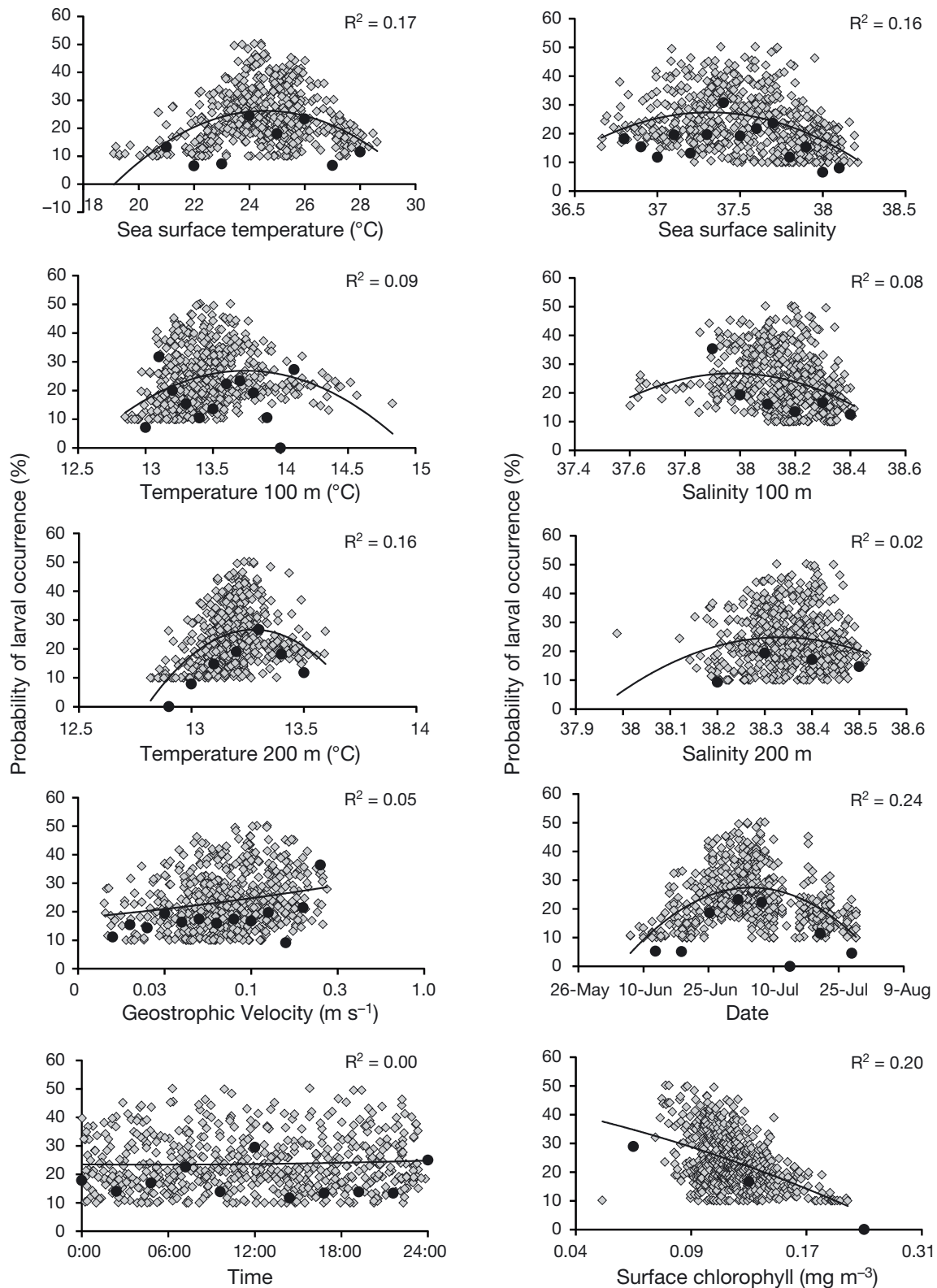


Fig. 7. Scatterplots of environmental variables and predicted probabilities of occurrence from the neural network model for the Balearic Islands. The general nature of the relationship between larval occurrences and each variable are shown using polynomial lines of best fit (black line). Observed proportions of stations with >0 bluefin tuna larvae are also shown in solid black dots, for binned environmental variables. Note nonlinear scales for surface chlorophyll and geostrophic velocities

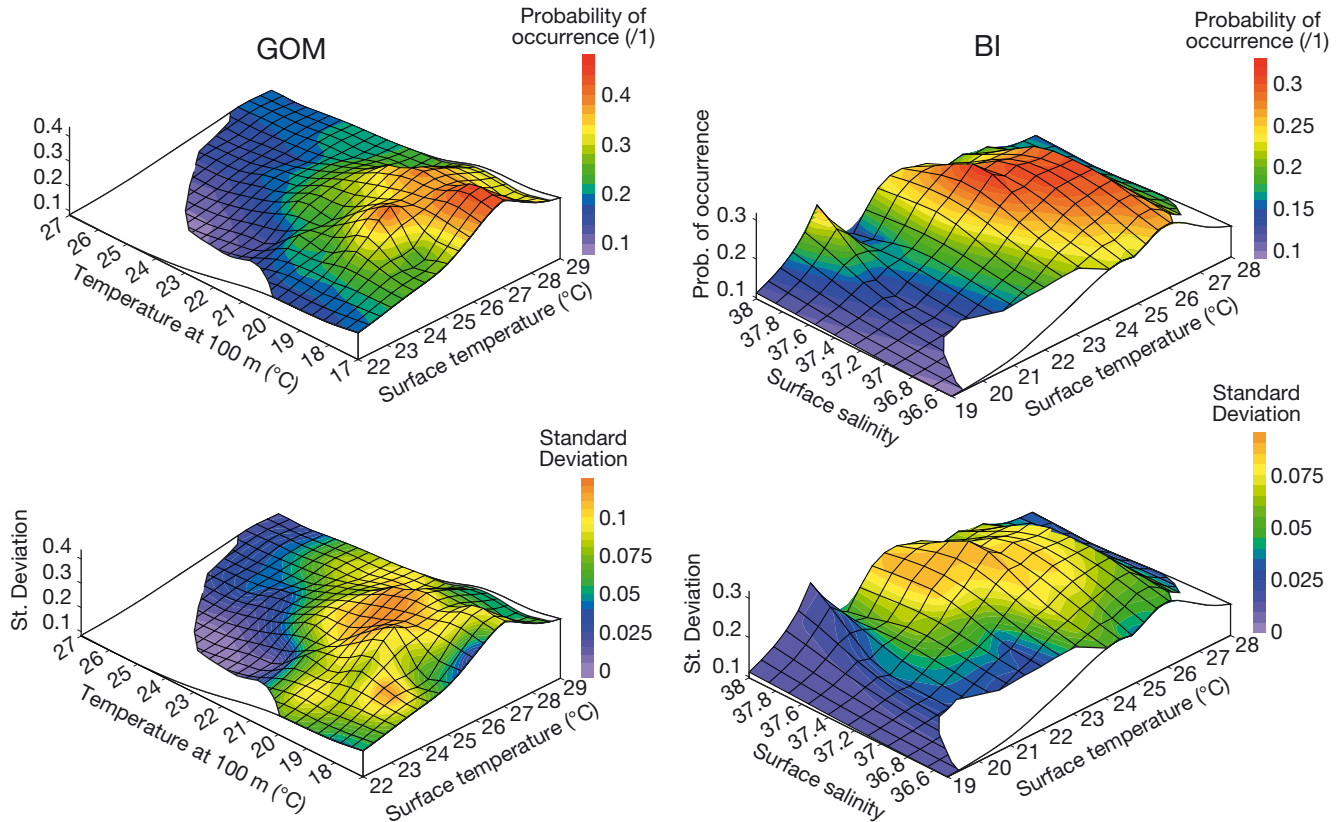


Fig. 8. Wireframe plots of mean modeled probabilities of larval bluefin tuna occurrence with surface temperature and temperature at 100 m in the Gulf of Mexico (left), and surface temperature and salinity in the Balearic Islands (right). Grid points with less than 4 observations have been blanked out. Standard deviations per grid point are also shown (bottom)

When results of habitat models were applied to 2 example years in the GOM (1999 and 2006), most positive stations were placed into favorable habitat (Fig. 9). Two positive stations from 2006 were in less favorable habitat near the edges of the Loop Current and a warm eddy. The effect of mesoscale features on predicted probabilities was evident from plots of temperature at 100 m depth and geostrophic velocity. BFT larvae were generally collected outside of the Loop Current (indicated by temperatures at depth $<22^{\circ}\text{C}$ and geostrophic velocities $<\sim 0.25\text{ m s}^{-1}$) in 1999, and outside of the Loop Current and an associated eddy in 2006. Oceanographic conditions around the BI were more complex; however, the habitat model still successfully placed most positive stations into favorable habitat (Fig. 10). In 2004, the most favorable habitat was to the east of the study area, and most positive stations were found in this area. Conversely, in 2005, larval habitat was more favorable in the western portion of the study area, and larval distributions were shifted accordingly. Larvae were found within zones of low surface chlorophyll ($>0.15\text{ mg m}^{-3}$) in both 2004 and 2005. Contours of

surface salinity showed the delineation between lower salinity Atlantic water in the south of the study area and higher salinity resident water in the north. In both years, larvae were most abundant in moderate salinities (37.2 to 37.8), presumably close to water mass boundaries. Interestingly, surface chlorophyll values were at a minimum in the vicinity of the frontal zone.

DISCUSSION

Results from this study generally agreed well with previous published research, suggesting that BFT spawn in warm, oligotrophic, offshore areas within the GOM and western Mediterranean Sea (Block et al. 2005, Teo et al. 2007, Alemany et al. 2010, Muhling et al. 2010, 2012, Reglero et al. 2012). Spawning in both areas appeared to commence when surface temperatures were in the low 20s ($^{\circ}\text{C}$), peak around the mid-20s, and tail off at warmer temperatures, although sampling restrictions in the GOM made determination of the end of the spawning season

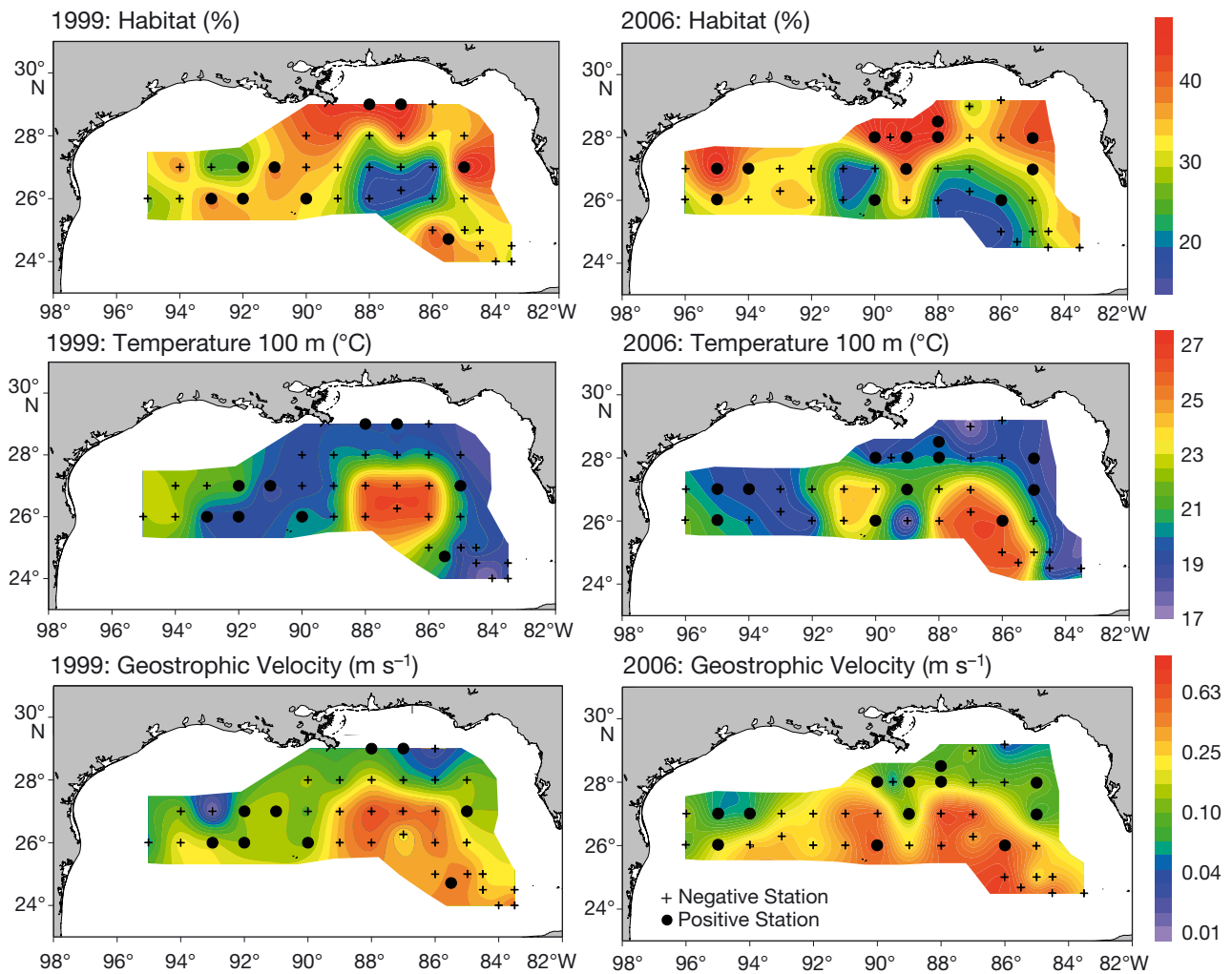


Fig. 9. Kriged predicted probabilities from neural network models of larval bluefin tuna occurrence for leg 2 of the 1999 and 2006 cruises in the Gulf of Mexico (top). All sampled stations, and larval bluefin tuna catch locations are indicated. Two environmental variables highlighted as influential in Fig. 6 are also shown: temperatures at 100 m depth in °C (middle), and geostrophic velocities in m s^{-1} (bottom), overlaid with larval catch locations. Note nonlinear (\log_{10}) scale for geostrophic velocities

there less certain. By the end of the spawning season, after approximately 6 to 8 wk, surface temperatures approach physiologically stressful values for adult BFT. At this time, adults presumably leave their spawning areas and migrate back to cooler feeding grounds in the North Atlantic (Block et al. 2005). Temperature stress may be more of a factor in the GOM, where surface temperatures during summer months reach 29 to 31°C, with no cooler waters nearby (Muller-Karger et al. 1991). As adult BFT show relatively shallow diving behavior in the GOM (Teo et al. 2007) and rarely cross the thermocline (Walli et al. 2009), their ability to avoid very warm waters in late spring and summer is limited. In contrast, the Mediterranean Sea stays cooler during the summer, particularly in the BI region. Although our study did not examine residence time on spawning grounds,

this is likely to be variable, with adult fish arriving and leaving throughout the spawning season (Farley & Davis 1998, Block et al. 2001, Galuardi et al. 2010).

A direct comparison of environmental conditions on both Atlantic spawning grounds revealed several similarities between the BI and GOM regions. In both areas, larvae were found in oligotrophic waters, even where higher productivity water masses were observed close by. This relationship was stronger in the BI than in the GOM, where lowest regional chlorophyll is usually within the Loop Current, which adult BFT avoid (Teo et al. 2007). Although the Mediterranean was much more saline than the GOM, larval distributions on both spawning grounds showed relationships with salinity. These were shown to be proxies for water mass: in the GOM, larval BFT were rarely collected within the Loop Current or warm

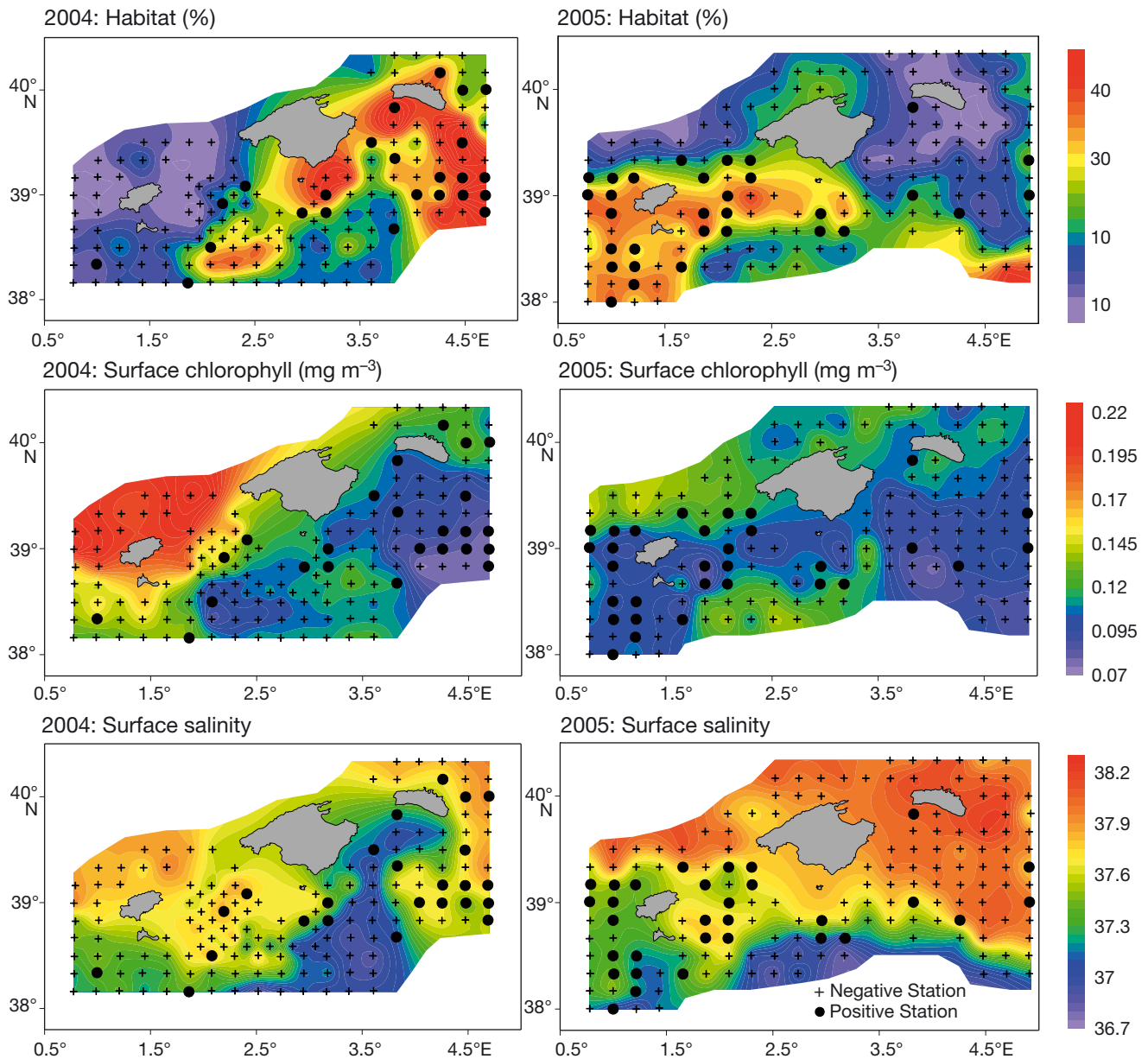


Fig. 10. Kriged predicted probabilities from neural network models of larval bluefin tuna occurrence for the 2004 and 2005 cruises in the Balearic Islands (top). All sampled stations, and larval bluefin tuna catch locations are indicated. Two environmental variables highlighted as influential in Fig. 6 are also shown: surface chlorophyll in mg m^{-3} (middle), and surface salinity (bottom), overlaid with larval catch locations

Loop Current eddies, which were best identified by elevated salinity and temperature at depth. In the BI, larvae were associated with moderate surface salinities around the frontal zone where less saline incoming Atlantic waters meet more saline resident waters. In both the GOM and BI, migrating adult BFT appeared to move past areas of very high current velocity, in the Loop Current and Alboran Sea respectively, and concentrate spawning in regions of moderate current flow ($<0.3 \text{ m s}^{-1}$). In the GOM, this corresponded to the offshore waters outside of high

chlorophyll continental shelf zones and large energetic eddy features. In the BI, larvae were concentrated near a frontal zone with low surface chlorophyll and no strong directional current flow.

Although larvae were found in 1 to 2°C cooler waters around the BI than in the GOM, it appears likely that temperature is an important physiological control in the initiation of spawning. In the Atlantic, Pacific and Indian oceans, temperature has been found to be a driving force behind spawning activity (Yukinawa 1987, Miyashita et al. 2000, Medina et al.

2002, Block et al. 2005, Tanaka et al. 2006, Alemany et al. 2010) and adult physiology (Carey & Teal 1966, Blank et al. 2004). Medina et al. (2002) suggested that water temperature triggers BFT spawning in the relatively short distance between the Straits of Gibraltar and the BI, although it remains unclear whether the absolute temperature or the rate of temperature increase is more important. Adult BFT in captivity have also been observed to spawn once water temperatures reach $\sim 22^{\circ}\text{C}$ (Sawada et al. 2005). Larval collections in both the Atlantic and Pacific oceans have mostly been restricted to waters between ~ 22 and 28°C (Masuma et al. 2006, Tanaka et al. 2006, Alemany et al. 2010, Muhling et al. 2010). Within the Mediterranean Sea, spawning takes place earlier in the eastern basin, where waters warm to suitable temperatures earlier in the year (Oray & Karakulak 2005). Egg hatching and larval development are also influenced by temperature, with around 25°C suggested to be optimal (Miyashita et al. 2000). Few studies exist on the effects of temperature on larval tuna growth, with some studies finding no association (Jenkins et al. 1991, Tanaka et al. 2006) and others a positive association (Reglero et al. 2011, Garcia et al. 2013). It may be that above a particular temperature threshold, larvae grow equally well, or that studies comparing temperatures across a broad enough range are lacking. Conversely, it is possible that concentrations of prey items typical of warm, oligotrophic waters are more influential in determining growth and survival than temperature itself. While moderately warm water temperatures appear to be required for spawning, the spatially and temporally restricted nature of spawning grounds and larval occurrences suggest that other biophysical factors are also important.

Studies concerning the diets of larval BFT are rare, but they appear likely to feed on copepods, copepod nauplii, cladocerans and appendicularians at preflexion stages, before becoming more piscivorous postflexion (Uotani et al. 1990, Llopiz et al. 2010, Catalán et al. 2011, Reglero et al. 2011). The advantages (if any) for larvae being spawned into oligotrophic regions remain unclear, although some hypotheses have been proposed. Bakun (2012) suggested that predation rates on larval BFT may be lower in less productive areas, and that the very high fecundity of adult BFT (Medina et al. 2002) may enable the overwhelming and satiation of resident planktonic predators by sheer numbers of spawned larvae. Oceanographic features such as eddies have been proposed as optimal spawning areas, providing locally enhanced feeding opportunities and sufficient

concentrations of tuna larvae to enable successful piscivory (Bakun 2012). In addition, spawning grounds may be characterized by optimal transport conditions for spawned larvae to nursery areas (Kitagawa et al. 2010). Results from this study found that larval densities in the GOM were lower in anticyclonic eddies, and in both the GOM and BI, larvae were not associated with strong, directional current flows. Although oceanographic conditions on BFT spawning grounds in the GOM, BI and the Pacific Ocean show several similarities, it would seem that adult BFT have modified their spawning strategies to best exploit local conditions. While entrainment in strong, directional flows may be beneficial for larvae if it facilitates delivery to nursery areas (Kitagawa et al. 2010), entrainment in the Loop Current (for example) would result in the rapid northwards transport of larvae in the Gulf Stream, away from assumed nursery areas in the GOM (Brothers et al. 1983). Similarly, while some mesoscale eddy features provide enhanced feeding and retention conditions for pelagic larvae (Bakun 2012), warm anticyclones may be much less beneficial than cooler cyclonic features. The complex mesoscale eddy fields in the western Mediterranean, resulting from inflowing Atlantic waters, contrast with the periodic shedding of large, warm anticyclonic eddies in the GOM (Milot, 1999, Lindo-Atichati et al. 2012), and both have different implications for larval feeding, transport and survival.

Larval BFT on both sides of the Atlantic appear to grow at around 0.3 to 0.4 mm per day during early life (Scott et al. 1993, Garcia et al. 2013), with a possible acceleration of growth associated with the onset of piscivory (Kaji et al. 1996, Tanaka et al. 2012). Some studies suggest that the fastest-growing larvae are most likely to ultimately survive, and therefore larvae which encounter conditions most conducive to rapid growth may be at an advantage (Brothers et al. 1983, Tanaka et al. 2006). However, larvae in high-density patches may grow more slowly due to density-dependent competition for prey (Jenkins et al. 1991). Improved understanding of ecological processes governing larval BFT growth and survival is clearly required before generalizations can be applied.

BFT larvae in both the GOM and BI were most likely to be collected in regions of moderate mesoscale oceanographic activity and eddy generation, but not in areas of strong, directional flow. In the BI, the salinity front between Atlantic and Mediterranean waters appeared most favorable. The strongest fronts in the GOM are associated with the Loop Current, and it has been suggested previously that

this region may be a focal point for spawning activity (Richards et al. 1989). However, adoption of a new, shallower sampling gear in the GOM in 2010 allowed improved assessment of the distribution of very small BFT larvae, and results showed that they were found across the northern GOM (Muhling et al. 2012). While it is possible that spawning in the GOM is associated with finer-scale fronts, eddies or other oceanographic features, the coarse nature of the Southeast Area Monitoring and Assessment Program sampling grid has not allowed thorough investigation of this. The habitat models described in this study are affected by several lags in time and space, as a result of temporal averaging and spatial interpolation of predictor variables, larval ages and larval patchiness. Larvae collected are probably several days to more than a week old, implying considerable drift since spawning. In addition, the scales of sampling are also likely to be much coarser than scales of larval patchiness. Allocation of spawning to finer-scale oceanographic features is therefore not possible at this stage, and will probably require a modified sampling design for both larvae and environmental variables.

Although this study concentrated on 2 well-known major spawning grounds for BFT, larvae have been collected in other locations. In the western Atlantic, at least some spawning activity appears to take place in the southern GOM and far west Caribbean Sea, although only very small numbers of larvae have been collected to date (Olvera-Limas et al. 1988, Muhling et al. 2011, National Oceanic and Atmospheric Administration National Marine Fisheries Service unpubl. data). The importance of the wider Caribbean Sea as a spawning area remains uncertain, although tagged fish have not been reported to travel south of Cuba on their way to the GOM. Parts of the western Caribbean are also warm to a greater depth than the northern GOM (Gordon 1967), which may inhibit the ability of adult fish to thermoregulate by diving. In the eastern Atlantic, BFT larvae have been collected in the far eastern Mediterranean Sea near Cyprus during June (Oray & Kurakulak 2005) and in the central Mediterranean during July (Tsuji et al. 1997, Koched et al. 2012). Tagged adult BFT have been shown to migrate from the open Atlantic into the Mediterranean as far as Sicily (Block et al. 2005), but migration patterns of fish spawning in the far eastern Mediterranean are less well known. They may not travel out to the Atlantic Ocean after spawning (De Metrio et al. 2004), but instead comprise a resident subpopulation. Druon et al. (2011) used remotely sensed surface temperatures and chloro-

phyll values to map potential spawning and feeding habitat for BFT in the entire Mediterranean Sea. Predicted suitable spawning locations from this study generally covered a greater spatial extent than confirmed spawning areas. This suggests that either additional environmental variables are important in determining actual spawning locations or that additional unconfirmed spawning areas exist.

Overall, this comparative study of environmental conditions on BFT spawning grounds in the GOM and BI suggested several strong similarities, including a preference for low chlorophyll ($<0.2 \text{ mg m}^{-3}$), warm waters (24 to 27°C) with moderate current flows ($<0.3 \text{ m s}^{-1}$) and high oceanographic complexity. Despite regional differences in water properties, observed relationships with salinity and with temperatures at depth were useful in defining water masses targeted for spawning. However, to elucidate the ecological implications of larvae spawned into these conditions, further research of adult reproductive systems, larval diets, growth, behavior and structure of planktonic food webs is clearly required. While modeling and conceptual studies are valuable, data on basic larval processes are lacking. In addition, identification of actual spawning locations through collections of eggs, larval backtracking studies or observations of spawning adults would be of great benefit in determining the precise conditions required for spawning. Nevertheless, the work described here comprises an important first step in the search for understanding the spawning ecology of BFT.

Acknowledgements. In the Balearic Islands, initial work was funded by the BALEARES project (CTM 2009-07944 MAR) and ATAME, 2011-29525-004-02, with base data provided by the TUNIBAL project (REN 2003-01176), which were competitive projects of the Spanish Government I+D+I (Research + Development + Innovation) National Plan. We also express our gratitude to the crew of the RV 'Vizconde de Eza' (2001 to 2002) and RV 'Cornide de Saavedra' (2003 to 2005), and to all the scientific staff that participated in surveys and carried out lab analysis, especially D. Cortés, T. Ramírez, M. Fernández de Puellas, J. Jansà, P. Vélez-Belchi, J. M. Rodríguez and C. González Pola. Special thanks are also extended to A. García and J. L. López Jurado, for their crucial role in the development of the TUNIBAL project. The authors also thank staff at the Sea Fisheries Institute Plankton Sorting and Identification Center, Gdynia and Szczecin, Poland, including M. Konieczna and L. Ejsymont, for processing of plankton samples from the Gulf of Mexico. We also extend our gratitude to all the captains and crew of all the NOAA ships who collected data on SEAMAP plankton cruises. Staff at the Early Life History laboratory of NOAA in Miami are thanked for collaboration, advice and data processing, in particular W. J. Richards, J. Roberts and the Marine Geospatial Ecology Toolbox at Duke University were immensely helpful for processing remotely sensed

environmental data. L.C. acknowledges further support from NSF-CMG grant 0934961. B.M. acknowledges the NASA Climate and Biological Response: Research and Applications program. D.A. was supported by the ICTS-SOCIB (focus research program bluefin tuna).

LITERATURE CITED

- Alemaný F, García A, González-Pola C, Jansa J, López Jurado JL, Rodríguez JM, Velez Belchi P (2010) Atlantic bluefin tuna and related species spawning habitat characterization: influence of environmental factors on larval abundance and distribution off Balearic archipelago (western Mediterranean). *Prog Oceanogr* 86:21–38
- Azov Y (1991) Eastern Mediterranean—a marine desert? *Mar Pollut Bull* 23:225–232
- Bakun A (2012) Ocean eddies, predator pits and bluefin tuna: implications of an inferred 'low risk–limited payoff' reproductive scheme of a (former) archetypical top predator. *Fish Fish*, doi:10.1111/faf.12002
- Blank JM, Morrisette JM, Landeira-Ferandez AM, Blackwell SB, Williams TD, Block BA (2004) *In situ* cardiac performance of Pacific bluefin tuna hearts in response to acute temperature change. *J Exp Biol* 207:881–890
- Block BA, Dewar H, Blackwell SB, Williams TD and others (2001) Migratory movements, depth preferences and thermal biology of Atlantic bluefin tuna. *Science* 293:1310–1314
- Block BA, Teo SLH, Walli A, Boustany A and others (2005) Electronic tagging and population structure of Atlantic bluefin tuna. *Nature* 434:1121–1127
- Brothers EB, Prince ED, Lee DW (1983) Age and growth of young-of-the-year bluefin tuna, *Thunnus thynnus*, from otolith microstructure. In: Prince ED, Pulos LM (eds) Proceedings of the international workshop on age determination of oceanic pelagic fishes: tunas, billfishes and sharks. NOAA Tech Rep NMFS 8:49–59
- Carey FG, Teal JM (1966) Heat conservation in tuna fish muscle. *Proc Natl Acad Sci USA* 56:1464–1469
- Castro LR, Salinas GR, Hernández EH (2000) Environmental influences on winter spawning of the anchoveta *Engraulis ringens* off central Chile. *Mar Ecol Prog Ser* 197:247–258
- Catalán IA, Tejedor A, Alemaný F, Reglero P (2011) Trophic ecology of Atlantic bluefin tuna *Thunnus thynnus* larvae. *J Fish Biol* 78:1545–1560
- Chase BC (2002) Differences in diet of Atlantic bluefin tuna (*Thunnus thynnus*) at five seasonal feeding grounds on the New England continental shelf. *Fish Bull* 100:168–180
- Clarke KR, Gorley RN (2006) PRIMER v6: user manual/tutorial. PRIMER-E, Plymouth
- Corten A (2001) The role of 'conservatism' in herring migrations. *Rev Fish Biol Fish* 11:339–361
- Cury P (1994) Obstinate nature: an ecology of individuals. Thoughts on reproductive behavior and biodiversity. *Can J Fish Aquat Sci* 51:1664–1673
- De Metrio G, Oray I, Arnold GP, Lutcavage M and others (2004) Joint Turkish-Italian research in the eastern Mediterranean: bluefin tuna tagging with pop-up satellite tags. *Collect Vol Sci Pap ICCAT* 56:1163–1167
- Druon JN, Fromentin JM, Florian A, Jukka H (2011) Potential feeding and spawning habitats of Atlantic bluefin tuna in the Mediterranean Sea. *Mar Ecol Prog Ser* 439:223–240
- Estrada M (1996) Primary production in the northwestern Mediterranean. *Sci Mar* 60:55–64
- Estrada JA, Lutcavage M, Thorrold SR (2005) Diet and trophic position of Atlantic bluefin tuna (*Thunnus thynnus*) inferred from stable carbon and nitrogen isotope analysis. *Mar Biol* 147:37–45
- Farley JH, Davis TLO (1998) Reproductive dynamics of southern bluefin tuna, *Thunnus maccoyii*. *Fish Bull* 96:223–236
- Fromentin JM, Powers JE (2005) Atlantic bluefin tuna: population dynamics, ecology, fisheries and management. *Fish Fish* 6:281–306
- Galuardi B, Royer F, Golet W, Logan J, Neilson J, Lutcavage M (2010) Complex migration routes of Atlantic bluefin tuna (*Thunnus thynnus*) question current population structure paradigm. *Can J Fish Aquat Sci* 67:966–976
- García A, Alemaný F, Velez-Belchi P, López Jurado JL and others (2005) Characterization of the bluefin tuna spawning habitat off the Balearic archipelago in relation to key hydrographic features and associated environmental conditions. *Collect Vol Sci Pap ICCAT* 58:535–549
- García A, Cortes D, Quintanilla J, Ramirez T, Quintanilla L, Rodríguez JM, Alemaný F (2013) Climate-induced environmental conditions influencing interannual variability of Mediterranean bluefin (*Thunnus thynnus*) larval growth. *Fish Oceanogr* 22:273–287
- Gardner MW, Dorling SR (1998) Artificial neural networks (the multilayer perceptron)—a review of applications in the atmospheric sciences. *Atmos Environ* 32:2627–2636
- Gilbes F, Tomas C, Walsh JJ, Muller-Karger FE (1996) An episodic chlorophyll plume on the West Florida Shelf. *Cont Shelf Res* 16:1201–1207
- Gordon AL (1967) Circulation of the Caribbean Sea. *J Geophys Res* 72:6207–6223, doi:10.1029/JZ072i024p06207
- Graham JB, Dickson KA (2004) Tuna comparative physiology. *J Exp Biol* 207:4015–4024
- Ingram GW Jr, Richards WJ, Lamkin JT, Muhling BA (2010) Annual indices of Atlantic bluefin tuna (*Thunnus thynnus*) larvae in the Gulf of Mexico developed using delta-lognormal and multivariate models. *Aquat Living Resour* 23:35–47
- International Commission for the Conservation of Atlantic Tunas (2011) Report of the 2010 Atlantic bluefin tuna assessment session. *Collect Vol Sci Pap ICCAT* 66:505–714
- Jenkins GP, Young JW, Davis TLO (1991) Density dependence of larval growth of a marine fish, the southern bluefin tuna, *Thunnus maccoyii*. *Can J Fish Aquat Sci* 48:1358–1363
- Kaji T, Tanaka M, Takahashi Y, Oka M, Ishibashi N (1996) Preliminary observations on development of Pacific bluefin tuna *Thunnus thynnus* (Scombridae) larvae reared in the laboratory, with special reference to the digestive system. *Mar Freshw Res* 47:261–269
- Kitagawa T, Kato Y, Miller MJ, Sasai Y, Sasaki H, Kimura S (2010) The restricted spawning area and season of Pacific bluefin tuna facilitate use of nursery areas: a modeling approach to larval and juvenile dispersal processes. *J Exp Mar Biol Ecol* 393:23–31
- Koched W, Hattour A, Alemaný F, García A, Said K (2012) Spatial distribution of tuna larvae in the Gulf of Gabes (eastern Mediterranean) in relation with environmental parameters. *Medit Mar Sci* 41:5–14
- Landaeta MF, Castro LR (2002) Spring spawning and early nursery zone of the mesopelagic fish *Maurolicus parvi-*

- pinnis* at the coastal upwelling zone off Talcahuano, central Chile. *Mar Ecol Prog Ser* 226:179–191
- Lindo-Atichati D, Bringas F, Goni G, Muhling B, Muller-Karger FE, Habtes S (2012) Varying mesoscale structures influence larval fish distribution in the northern Gulf of Mexico. *Mar Ecol Prog Ser* 463:245–257
- Llopiz JK, Richardson DE, Shiroza A, Smith SL, Cowen RK (2010) Distinctions in the diets and distributions of larval tunas and the important role of appendicularians. *Limnol Oceanogr* 55:983–996
- Malmgren BA, Winter A (1999) Climate zonation in Puerto Rico based on principal components analysis and an artificial neural network. *J Clim* 12:977–985
- Masuma S, Tezuka N, Koiso M, Jinbo T and others (2006) Effects of water temperature on bluefin tuna spawning biology in captivity. *Bull Fish Res Agency* 4(Suppl): 157–172
- Medina A, Abascal FJ, Megina C, Garcia A (2002) Stereological assessment of the reproductive status of female Atlantic northern bluefin tuna during migration to Mediterranean spawning grounds through the Strait of Gibraltar. *J Fish Biol* 60:203–217
- Millot C (1999) Circulation in the western Mediterranean Sea. *J Mar Syst* 20:423–442
- Miyashita S, Yuji T, Yoshifumi S, Osamu M, Nobuhiro H, Kenji T, Toshio M (2000) Embryonic development and effects of water temperature on hatching of the bluefin tuna, *Thunnus thynnus*. *Suisan Zoshoku* 48:199–207
- Motos L, Uriate A, Valencia V (1996) The spawning environment of the Bay of Biscay anchovy (*Engraulis encrasicolus* L.). *Sci Mar* 60:117–140
- Muhling BA, Lamkin JT, Roffer MA (2010) Predicting the occurrence of bluefin tuna (*Thunnus thynnus*) larvae in the northern Gulf of Mexico: building a classification model from archival data. *Fish Oceanogr* 19:526–539
- Muhling BA, Lamkin JT, Quattro JM, Smith RH, Roberts MA, Roffer MA, Ramirez K (2011) Collection of larval bluefin tuna (*Thunnus thynnus*) outside documented western Atlantic spawning grounds. *Bull Mar Sci* 87: 687–694
- Muhling BA, Roffer MA, Lamkin JT, Ingram GW Jr and others (2012) Overlap between Atlantic blue n tuna spawning grounds and observed Deepwater Horizon surface oil in the northern Gulf of Mexico. *Mar Pollut Bull* 64:679–687
- Muller-Karger FE, Walsh JJ, Evans RH, Meyers MB (1991) On the seasonal phytoplankton concentration and sea surface temperature cycles of the Gulf of Mexico as determined by satellites. *J Geophys Res Oceans* 96: 12645–12665
- Neumann DE (2002) An enhanced neural network technique for software risk analysis. *IEEE Trans Softw Eng* 28:904–912
- Olden JD, Lawler JJ, Poff NL (2008) Machine learning methods without tears: a primer for ecologists. *Q Rev Biol* 83: 171–193
- Olvera Limas R, Cerecedo JL, Compean GA (1988) Distribucion de larvas de tunidos en el Golfo de Mexico y Mar Caribe: abundancia y biomasa de tres especies en la zona economica exclusiva. *Cienc Pesq* 6:119–140
- Oray IK, Karakulak FS (2005) Further evidence of spawning of bluefin tuna (*Thunnus thynnus* L., 1758) and the tuna species (*Auxis rochei* Ris., 1810, *Euthynnus alletteratus* Raf., 1810) in the eastern Mediterranean Sea: preliminary results of TUNALEV larval survey in 2004. *J Appl Ichthyology* 21:236–240
- Reglero P, Urtizberea A, Torres AP, Alemany F, Fiksen O (2011) Cannibalism among size classes of larvae may be a substantial mortality component in tuna. *Mar Ecol Prog Ser* 433:205–219
- Reglero P, Cianelli L, Alvarez-Berastegui D, Balbín R, López-Jurado JL, Alemany F (2012) Geographically and environmentally driven spawning distributions of tuna species in the western Mediterranean Sea. *Mar Ecol Prog Ser* 463:273–284
- Richards WJ, Leming T, McGowan MF, Lamkin JT, Kelley-Fraga S (1989) Distribution of fish larvae in relation to hydrographic features of the Loop Current boundary in the Gulf of Mexico. *Rapp Cons Int Explor Mer* 191:169–176
- Roberts JJ, Best BD, Dunn DC, Treml EA, Halpin PN (2010) Marine Geospatial Ecology Tools: an integrated framework for ecological geoprocessing with ArcGIS, Python, R, MATLAB, and C++. *Environ Model Softw* 25: 1197–1207
- Rooker JR, Bremer JRA, Block BA, Dewar H and others (2007) Life history and stock structure of Atlantic bluefin tuna (*Thunnus thynnus*). *Rev Fish Sci* 15:265–310
- Rooker JR, Secor DH, De Metrio G, Schloesser R, Block BA, Neilson JD (2008) Natal homing and connectivity in Atlantic bluefin tuna populations. *Science* 322:742–744
- Roy C (1998) An upwelling-induced retention area off Senegal: a mechanism to link upwelling and retention processes. *S Afr J Mar Sci* 19:89–98
- Sawada Y, Okada T, Miyashita S, Murata O, Kumai H (2005) Completion of the Pacific bluefin tuna *Thunnus orientalis* (Temminck et Schlegel) life cycle. *Aquacult Res* 36: 413–421
- Schaefer KM (2001) Reproductive biology of tunas. In: Block BA, Stevens ED (eds) *Tuna: physiology, ecology, and evolution*. Academic Press, San Diego, CA, p 225–270
- Scott GP, Turner SC, Grimes CB, Richards WJ, Brothers EB (1993) Indices of larval bluefin tuna, *Thunnus thynnus*, abundance in the Gulf of Mexico: modeling variability in growth, mortality, and gear selectivity: ichthyoplankton methods for estimating fish biomass. *Bull Mar Sci* 53: 912–929
- Segurado P, Araujo MB (2004) An evaluation of methods for modelling species distributions. *J Biogeogr* 31:1555–1568
- Shanks AL, Eckert GL (2005) Population persistence of California current fishes and benthic crustaceans: a marine drift paradox. *Ecol Monogr* 75:505–524
- Sherman K, Smith W, Morse W, Berman M, Green J, Ejsymont L (1984) Spawning strategies of fishes in relation to circulation, phytoplankton production, and pulses in zooplankton off the northeastern United States. *Mar Ecol Prog Ser* 18:1–19
- Sherrod PH (2003) DTREG: classification and regression trees for data mining and modeling. Available at www.dtregr.com/DTREG.pdf, accessed September 2012
- Sims DW, Wearmouth VJ, Genner MJ, Southward AJ, Hawkins SJ (2004) Low-temperature-driven early spawning migration of a temperate marine fish. *J Anim Ecol* 73:333–341
- Sinclair M, Iles TD (1985) Atlantic herring (*Clupea harengus*) distributions in the Gulf of Maine—Scotian Shelf area in relation to oceanographic features. *Can J Fish Aquat Sci* 42:880–887
- Sousa SIV, Martins FG, Alvim-Ferraz MCM, Pereira MC (2007) Multiple linear regression and artificial neural networks based on principal components to predict ozone concentrations. *Environ Model Softw* 22:97–103

- Stokesbury MJW, Teo SLH, Seitz A, O'Dor RK, Block BA (2004) Movement of Atlantic bluefin tuna (*Thunnus thynnus*) as determined by satellite tagging experiments initiated off New England. *Can J Fish Aquat Sci* 61: 1976–1987
- Tanaka Y, Satoh K, Iwahashi M, Yamada H (2006) Growth-dependent recruitment of Pacific bluefin tuna *Thunnus orientalis* in the northwestern Pacific Ocean. *Mar Ecol Prog Ser* 319:225–235
- Tanaka Y, Minami H, Ishihi Y, Kumon K and others (2012) Relationship between prey utilization and growth variation in hatchery-reared Pacific bluefin tuna, *Thunnus orientalis* (Temminck et Schlegel), larvae estimated using nitrogen stable isotope analysis. *Aquacult Res*, doi: 10.1111/j.1365-2109.2012.03258.x
- Teo SLH, Boustany AM, Dewar H, Stokesbury MJW and others (2007) Annual migrations, diving behavior, and thermal biology of Atlantic bluefin tuna, *Thunnus thynnus*, on their Gulf of Mexico breeding grounds. *Mar Biol* 151:1–18
- Torres AP, Reglero P, Balbin R, Urtizberea A, Alemany F (2011) Coexistence of larvae of tuna species and other fish in the surface mixed layer in the NW Mediterranean. *J Plankton Res* 33:1793–1812
- Tsuji S, Nishikawa Y, Segawa K, Hiroe Y (1997) Distribution and abundance of *Thunnus* larvae and their relation to the oceanographic condition in the Gulf of Mexico and the Mediterranean Sea during May through August of 1994 (draft). *Collect Vol Sci Pap ICCAT* 46:161–176
- Uotani I, Saito T, Hiranuma K, Nishikawa Y (1990) Feeding habit of bluefin tuna *Thunnus thynnus* larvae in the western North Pacific Ocean. *Nippon Suisan Gakk* 56: 713–717
- Walczak S, Cerpa N (1999) Heuristic principles for the design of artificial neural networks. *Inf Softw Technol* 41: 107–117
- Walli A, Teo SLH, Boustany A, Farwell CJ and others (2009) Seasonal movements, aggregations and diving behavior of Atlantic bluefin tuna (*Thunnus thynnus*) revealed with archival tags. *PLoS ONE* 4:e6151
- Wilson SG, Lutcavage ME, Brill RW, Genovese MP, Cooper AB, Everly AW (2005) Movements of bluefin tuna (*Thunnus thynnus*) in the northwestern Atlantic Ocean recorded by pop-up satellite archival tags. *Mar Biol* 146: 409–423
- Yukinawa M (1987) Report on the 1986 research cruise of the R/V Shoyo Maru. Distribution of tuna and billfishes larvae and oceanographic observation in the eastern Indian Ocean January–March 1987. *Rep Res Div Fish Agency Jpn* 61:1–100

Editorial responsibility: Nicholas Tolimieri, Seattle, Washington, USA

*Submitted: February 11, 2013; Accepted: April 30, 2013
Proofs received from author(s): July 5, 2013*